A semi-automated design for high-throughput Lepidoptera larvae feeding bioassays

Inoussa Sanané[1&2], Judith Legrand[1], Christine Dillmann[1], Frédéric Marion-Poll[2]

(1) Université Paris-Saclay, INRAE, CNRS, AgroParisTech, GQE - Le Moulon, 91190, Gif-sur-Yvette, France.

(2) Université Paris-Saclay, CNRS, IRD, UMR Évolution, Génomes, Comportement et Écologie, 91198, Gif-sur-Yvette, France.

Abstract

Lepidopteran pests cause considerable damage to all crops over the world. As larvae are directly responsible for these damages, many research efforts are devoted to find plant cultivars which are resistant against them. However, such studies take time, efforts and are costly, especially when one wants to not only find resistance traits but also evaluate their heritability. We present here a high throughput approach to screen plants for resistance or chemicals for their deterrence, using a leaf-disk consumption assay, which is both suitable for large scale tests and economically affordable. To monitor larvae feeding on leaf disks placed over a layer of agar, we designed 3D models of 50 cages arrays. One webcam can sample simultaneously 3 of such arrays at a rate of 1 image/min, and follow individual feeding activities in each cage as the movements of 150 larvae. The resulting image stacks are first processed with a custom program running under an open-source image analysis package (Icy) to measure the surface of each leaf disk over time. We further developed statistical procedures running under the R package, to analyze the time course of the feeding activities of the larvae and to compare them between treatments. As a test case, we compared how European corn borer larvae respond to quinine, considered as a bitter alkaloid for many organisms, and to Neemazal containing azadirachtin,

which is a common antifeedant against pest insects. We found that increasing doses of azadirachtin reduce and delay feeding. However, contrary to our expectation, quinine was found poorly effective at the range of concentrations tested. The 3D printed model of the cage, of the camera holder, the plugins running under Icy, and the R procedures are freely available, and can be modified according to the particular needs of the users.

Keys words: plant-insect warfare, feeding preferences, digital image analysis, high-throughput device

Introduction

Our crops are exposed to increased pressure from insect pests. This increased pressure of pests is partly due to the climate warming, which changes the distribution of pest insects [1,2]. It is also a consequence of the globalization of our economies, which allow pests to cross natural barriers and invade new ecosystems, causing massive direct and indirect costs to our economies [3]. Such pests often become invasive because they lack their usual natural enemies, they face plants which may have poor defenses against them [4], and when confronted to new biotic and abiotic conditions, they may become more adaptable [5]. Invasive pests require not only swift detection and containment measures to contain their spread but also to quickly design new means to protect the cultures [4].

To cope with such pests, it is most effective to use or develop resistant or tolerant crop varieties, but the whole process is both costly and time-consuming [6]. High-throughput laboratory assays are thus needed to find plants potentially carrying resistance traits, within traditionally bred varieties or material derived from global germplasm. This can be done either by growing plants in a field or in a controlled environment and then measuring the impact of specific pests on the final yield, or it can be done on plant organs exposed to the pest.

Leaf-disk assays are commonly used to evaluate plant resistance against insects with chewing mouthparts [7,8] by measuring the area of tissues consumed. They can be used also on mites, thrips, aphids, whiteflies, or even fungi by monitoring visual changes related to the damaged areas of the leaves [9]. While disk assays have drawbacks such as the damage inflicted to the tissue, several studies demonstrate that resistance scores obtained using this approach are comparable to those completed on detached or attached leaves [9].

Leaf-disk assays are particularly well adapted to evaluate antibiosis factors against Lepidoptera larvae feeding on leaves. They are even relevant to larvae feeding within the stem because adult females deposit their eggs on the plant surface. Therefore, first instar larvae hatching from the eggs need to graze on the leaf surface, and bore a tunnel through the leaves to reach the inner tissues. Leaf-consumption by young larvae can thus be used as a proxy to evaluate plant resistance, and to find and evaluate the effectiveness of feeding deterrents extracted from plants or of synthetic origin [10–14].

So far, very few systems have been described to perform such tests on large numbers of insects at once. Most experimental setups used image analysis to measure leaf disk area consumed by larvae either visually [7,10], or digitally [15–19]. These approaches are well suited to laboratory investigations on small scale series, but handle a limited number of repetitions and often make use of specialized and expensive hardware.

We describe here a fast and reliable testing protocol that can be performed using a minimum of hardware components, based upon measuring the consumption of leaf disks by larvae. Our approach combines three elements (i) a novel and flexible feeding bioassay whereby the consumption and movements of 150 larvae can be followed across several days with a webcam, (ii) programs to analyze the stacks of images (RoitoRoiArray and AreaTrack), written as plugins running within the free bio-image software ICY [20] , and (iii) a new cutting-edge statistical approach to compare the kinetics of larval feeding, taking into account the diversity

of behavioral responses in the insect population. As an example, we monitored the feeding behavior of European corn borer (ECB) second instar larvae on maize leaf disks treated with different doses of neem oil and of quinine, which are considered as antifeedants for a number of insect species.

Results

The typology of feeding behaviours results from a novel, high-throughput feeding bioassay

We designed a high-throughput feeding bioassay to analyse the feeding behaviour of second instar larvae (L2) from European corn borer *Ostrinia nubilalis* Hübner (Lepidoptera: Crambidae) on maize leaf disks. We examined the feeding behaviour of cohorts of larvae given access to maize disks treated with different amounts of two antifeedant molecules. Although considerable variation exists between larvae, we showed that their behaviour can be classified into six categories (behavioural types). Differences between behavioural types relate to the time to engage into sustained consumption and to their consumption rate. The building-up of behavioural typologies relies on three innovations:

A custom recording system: Each recording unit (Fig 1) includes three plates of 50 cages, placed over a white LED panel and monitored by a webcam mounted on a custom stand. The bottom of each plate is made of a transparent glass plate. Each cage is first filled with a 2-3 mm layer of agar on which a freshly cut leaf-disk is deposited. Then one larva is placed in each cage and second a glass plate is placed on the top to close the cage. The cost of one system is less than 400 $ US. The camera can record images at regular intervals (1 per minute) using a surveillance camera security software (VisionGS). As introducing insect larvae into the cages was time consuming, one operator alone could start only 1 experiment at a time. This allowed us to register the feeding behaviours of 150 larvae, distributed into three plates/treatments,

during several days. One standard computer could easily control 4 webcams that is to say it's can be possible to record feeding bioassay test with 600 larvae at a time on one computer.

Fig 1. Feeding bioassay device for real-time image video recording. A_One feeding bioassay comprises one batch with three 50-cages plates numbered a, b, c and a webcam that is connected to a computer for image registration; B_Plate from profile cover with two transparent glass that shows larvae on feeding during device running. C_One plate consists in 150 cages, each representing an experimental unit.

Open-source software for image analysis: The analysis of the image stacks (1920 x 1080 pixels; RGB 24 bits) is performed with 2 plugins written in Java, and running (Fig 2) under the open-source bio-imaging software, Icy [20]. A first plugin, RoitoRoiArray is used to help users to create areas defining the contour of each cage, and attributing them a unique ID number. A second plugin, AreaTrack is used to measure the leaf area along time. Leaves are isolated from the background, either with a set of pre-defined image filters transforming the image into a grey image on which a simple threshold is applied, or with user-defined arrays of colours. The number of pixels matching these filters is monitored over time and exported as a csv file.

Fig 2. Image analysis plugins. (a&b) RoitoRoiArray automatically delimits the cages using the first picture. (c&d) AreaTrack convert pixels within each cage and measures intact leaf disks area at each time point. Main steps of both algorithms are described in (a&c). Outputs are csv files with leaf areas recorded every minute.

Freely-available R-scripts for data-processing and model-based data analysis: One experiment consists in several bioassays where the statistical unit is a curve corresponding to the consumption of a single leaf disk measured through time (Fig 3.1). The different steps including data processing and data analysis were encoded into R scripts that are freely available, along with the user manual.

Fig 3. Data processing. 3.1 Raw data processing. Images are converted into (i) a pile of pdf files that allows the manual checking of the consumption curves and (ii) R data frames were each observation is one consumption curve. **3.2 Unsupervised clustering.** SOTA classification into 14 clusters. For each cluster found by SOTA, the median consumption curve is represented by a color line. At each time point, range of variation around the median within the cluster is represented by a grey area. **3.3 Typology of feeding behaviours.** Each cluster was characterized by its median value concerning t20, t50, t80 and total consumption. A K-means algorithm was run to attribute the 14 clusters into six behavioural types. **3.3 Right.** The 14 clusters are represented on the first two axes of a principal component analysis based on median behavioural traits. K-means behavioural types are mainly explained by traits correlated to PCA axis 1 (t80, t50), except for behavioural types B and C that differ for t20. **3.3 Left.** Barplot of median behavioural traits (t20, t50, t80) for each behavioural type and each SOTA cluster within behavioural type. **3.4 Differences between treatments for the distribution of behavioural types.** Raw data contingency tables are represented as pie chart for three different treatments: Neemazal 10mM, Water (control), and Quinine 100mM.

The SOTA algorithm (Self Organizing Tree Algorithm) is an unsupervised neural network associated with a binary tree topology in which terminal nodes are the resulting clusters. It is particularly adapted to the classification of temporal data and allowed us to group individual

data into 14 different clusters (Fig 3.2). As shown in Figure 3.2, differences between individual behaviours and the cluster median are moderate. Each cluster was further characterized by behavioural traits like the time to consume 20%, 50% or 80% of the leaf disk, as well as the total consumption at the end of the experiment. Behavioural traits were used to group the 14 clusters into six behavioural types (Figs 3.2 and 3.3):

- A-type larvae immediately start to feed (low t20), consume fast (low t50, t80) and finish the leaf disk before the end of the experiment.
- B-type larvae tend to wait before consuming (high t20) but consume fast after the waiting time and generally consume all the leaf disk.
- C-type larvae consume fast in the beginning (low t20) but reduce their consumption rate through time, resulting in low t50 but high t80.
- D-type larvae show a behaviour intermediate between B and C, with high t20 and high t50.
- E-type larvae are reluctant to start feeding, showing high t20, t50 and t80, but achieving a significant consumption at the end.
- F-type larvae do not consume the leaf disk.

At the end, each individual data can be attributed a single behavioural type. The comparison between treatments result in comparisons between the proportions of each behavioural type within each treatment (Fig 3.4). Fig 3.4. shows that when maize leaves are treated with water, most larvae choose the A or B feeding behaviour and consume the maize disk fast. The treatment with 100mM quinine gives almost the same results. However, when maize leaves are treated with 10mM NeemAzal, most of the larvae do not consume the leaves and are classified into the F behavioural type. Further, the classification of each individual observation into six behavioural types allows to use multinomial regression to perform statistical tests and compare the different treatments.

Altogether, our experimental design revealed the diversity of behavioural responses of ECB larvae when feeding on maize leaf disks. Even without treatment, a proportion of the larvae decide not to eat. We propose here a statistical method to compare treatments considering the variability of individual behaviours. We defined a typology of possible behaviours taking into account the whole data set and compare the distribution of behavioural types between treatments.

Bioassays confirm NeemAzal as an antifeedant for ECB larvae

We ran a total of eight batches to compare the larvae responses to different concentrations of NeemAzal and quinine. After using the whole data set to attribute a behavioural type to each individual (Fig 3), the effect of each molecule was analysed separately. For both molecules, the multinomial regression chose the better model (based on AIC) as the one including treatment effect. The behavioural types were distributed differently between treatments, more than between plates, whatever the treatment (Tables 1 and 2). Fig 4 shows the estimations of the probability distribution among behavioural types for each concentration of each treatment.

Fig 4. Distribution of behavioural types along treatments. For each treatment (row), the estimated probability of each behavioural type is represented as a pie. Each row sums to one. (a) **Neemazal treatments**. The Neemazal concentrations are indicated in the row names. None correspond to the control with water. Neemazal concentrations are represented in the pies with red colours. (b) **Quinine treatments**. The Quinine concentrations are indicated in the row names. None correspond to the control with water. Quinine concentrations are represented in the pies with blue colours.

In the NeemAzal bioassay, an increasing concentration of the product is clearly associated with a decreasing proportion of A and B behavioural types, and an increasing proportion of E and F behavioural types (Fig 4a). Intermediate concentrations correspond to a higher proportion of C, D, E behavioural types. These results are confirmed by statistical tests (Table 1). All comparisons between 10 mM NeemAzal and lower concentrations are negative for behavioural types A, B, C, D, and positive for behavioural type F. Notice that for the B behavioural type, the comparisons lead to negative but non-significant contrasts. This may indicate a lack of power of th experimental design. According to Table 1, 0.1mM and 0.01mM NeemAzal treatments are generally non-significantly different from the control, except for behavioural types A, B C. Altogether, the data indicate that ECB larvae detect NeemAzal and change their feeding behaviour according to the concentration of the molecule. The higher the concentration, the lower the consumption.

Contrast	A	B	C	D	F
neem_10-3mM	-10,8	-8,32	2,165	-12,1	4,59
neem_10-1mM	-12,6	-11,3	-15,3	-14,4	4,78
nem_10-0,1mM	-15,3	-12,2	-16,2	-15	5
neem_10-0,01mM	-17,1	-14	-16,7	-15,3	4,88
neem_10mM-Control	-18,1	-15,3	-17,3	-15,1	2,75
neem_3-1mM	-1,77	-2,97	-17,5	-2,33	0,18
neem_3-0,1mM	-4,5	-3,93	-18,4	-2,87	0,41
neem_3-0,01mM	-6,29	-5,64	-18,9	-3,16	0,29
neem_3mM-Control	-7,23	-6,94	-19,5	-2,97	-1,85
neem_1-0,1mM	-2,73	-0,96	-0,91	-0,54	0,22
neem_1-0,01mM	-4,52	-2,67	-1,39	-0,83	0,11
neem_1mM-Control	-5,46	-3,97	-1,98	-0,64	-2,03
neem_0,1-0,01mM	-1,79	-1,71	-0,48	-0,29	-0,12
neem_0,1mM-Contol	-2,73	-3,01	-1,07	-0,1	-2,25
neem_0,01mM-Control	-0,94	-1,3	-0,59	0,183	-2,13

Table 1: Contrasts between the different concentrations of NeemAzal treatments within each typology of feeding behaviour. Contrasts are exprimed on the logit scale, relative to the reference feeding behavioural category E. For each contrast and each feeding category, the levels of significance is indicated by the colour filling. White = significant at the Bonferoni risk level. Lightgrey = significant at the 1% risk level. Darkgray = non significant at the 1% risk level.

In the quinine bioassay, we hardly saw any effect of concentration on the distribution of behavioural types, except for an excess of feeding types C, D, E in the 100mM treatment as compared to 10 mM (Fig 4b). This result is comforted by the comparison of means (Table 2). Even when leaf disks were treated with 100 mM Quinine, the proportion of larvae showing an A/B feeding behaviour was still elevated. This indicate that quinine, when diluted with water, has no effect on larvae feeding behaviour.

	A	B	C	D	E
quin_100-10mM	-1,3	-0,08	16,06	16,47	15,12
quin_100-1mM	0,14	0,49	0,742	0,657	1,099
quin_100-0,1mM	-1,94	-0,75	-0,42	1,216	0,118
quin_100-0,01mM	0,05	0,41	1,738	2,683	15,17
quin_100mM-Control	-0,62	0,55	-0,13	1,453	1,558
quin_10-1mM	1,44	0,57	-15,3	-15,8	-14
quin_10-0,1mM	-0,64	-0,67	-16,5	-15,3	-15
quin_10-0,01mM	1,35	0,49	-14,3	-13,8	0,054
quin_10mM-Control	0,68	0,63	-16,2	-15	-13,6
quin_1-0,1mM	-2,08	-1,24	-1,16	0,559	-0,98
quin_1-0,01mM	-0,1	-0,09	0,996	2,026	14,07
quin_1mM-Control	-0,76	0,05	-0,88	0,796	0,46
quin_0,1-0,01mM	1,98	1,15	2,16	1,467	15,05
quin_0,1mM-Control	1,32	1,29	0,288	0,237	1,441
quin_0,01mM-Control	-0,66	0,14	-1,87	-1,23	-13,6

Table 2: Contrasts between the different concentrations of Quinine treatments within each typology of feeding behaviour. Contrasts are exprimed on the logit scale, relative to the

reference feeding behavioural category F. For each contrast and each feeding category, the levels of significance is indicated by the colour filling. White = significant at the Bonferoni risk level. Lightgrey = significant at the 1% risk level. Darkgray = non significant at the 1% risk level.

Discussion

We describe here a high-throuput semi-automated design able to follow the feeding activities and movements of 150 larvae at a time using a single webcam. This system was built with on-the-shelf readily available elements and can be duplicated and adapted to different situations. While similar systems were proposed in the past, using videographic analyses to measure leaf consumption from a limited number of larvae, this is the first time such a system is demonstrated to run on such a large batch of insects. Such performances are made possible by the current evolution of the technology and because we chose to sample images at a relatively low frequency rate. Previously described approaches using videographic analyses were combining the measure of leaf areas with feeding phases and movements of the larvae, using movies acquired at 30 images per s from a single larva [19] or from a group of twelve larvae [17]. Actually, with this approach, the limiting factor is the time to prepare the setups, and more specifically, the time to collect the larvae and to introduce them into individual cages. If the whole process is performed by one operator at a time, it was found reasonable that each batch of experiments would be performed on 150 larvae.

One drawback of this method, is that the feeding activities are measured on excised tissue. This has three consequences. First, the excised tissue is deprived of its normal input of nutriments and it is prone to desiccation, changing its physiology and shape. Maintaining the moisture of leaf disks punched on the plant can limit desiccation during the experiment [16,19,21]. Second, the leaf disk characteristics change over the course of the experiment, their colour may turn yellowish or becoming paler. This is why we fill the cages with 1% agarose the day before the

experiment [21], and sandwich them between two glass plates as shown in Fig 1. Lastly, leaf disks are mechanically excised, thus wounding the tissues, especially along the border of the disk. As reported in [9], several studies found no differences between detached/attached leaves and leaf disc assays. The results obtained with leaf disks ought to be considered as a proxy precisely because of these limitations. Nevertheless, they are not only easy to carry, but since they allow a physical separation between the production of the plants and the location where the pest insects are held, it minimizes the risks of contamination of the plant production site.

As a test case, we analysed here how European corn borer larvae modulate their feeding activities when leaf disks are treated with of two potential antifeedants, NeemAzal which contains azadirachtin, and quinine which an alkaloid detected as bitter by many organisms including humans. Azadirachtin is a triterpenoid, and a complex molecule, which is often considered as a universal antifeedant for insects [22,23]. NeemAzal is a commercial extract containing mainly azadirachtin and it was previously shown that it is indeed antifeedant for ECB larvae [10,15], showing both antifeedant and insecticide activities [10,24,25]. We found here that NeemAzal has a strong impact on the distribution of consumption curves (Fig 4a). As another test compound, we chose the alkaloid quinine, which is found in the bark of *Cinchona* and *Remijia* trees [26]. This compound is used as an antimalarial agent and is used at low doses for its bitter taste to humans. It is antifeedant to a host of different animals, including *Drosophila [27]*, and several Lepidoptera [28–31]. Interestingly, ECB larvae did not respond to quinine in our tests. Scattered observations in the literature reported the absence of bitterness of quinine in another Lepidoptera [32] or mantids [33]. While this observation is new for *O. nubilalis*, it remains to be tested if the lack of response to quinine is species-specific. Actually, immature insect stages may exhibit different taste responses as shown in a Diptera [34] and one Lepidoptera [35], and this lack of sensitivity may concern only the specific larval stage (L2) tested here.

Our approach introduces a new analysis which is new for this field. We designed a rigorous statistical approach to compare the time course of feeding activities. Classical consumption tests usually rely upon comparing feeding after fixed interval(s) of time [10,11,16,36–40]. With the approach developed here, we can characterize properly the different feeding strategies adopted by groups of insects confronted to the same situation. While the classical approach and our approach may globally obtain comparable results, we will be able to better characterize if plant resistance factors or externally applied chemicals have an immediate sensory effect or if they are the consequence of post-ingestive effects.

Lastly, the system described here, with its cutting edge methodology, its affordability and its possibility to test large number of insects opens up new possibilities to evaluate the variability of feeding behaviours within populations of insects.

Materials and Methods

Insect rearing

Ostrinia nubilalis H. eggs were obtained from Bioline AgroSciences (France). Eclosed larvae were maintained in Petri dishes on an artificial diet (1.32 l water, 27 g agar powder, 224 g corn flour, 60 g dried yeast, 56 g wheat germ, 12 g L-ascorbic acid, 4 g vitamin mixture and minerals (Réf.0155200), 0.8 g chlortetracycline, 2 g hydroxybenzoic acid methyl, 1.6 g sorbic acid and 4 g benzoic acid), under 16 :8 (light: dark) photoperiod at 70% humidity and at 26°C. Second instar larvae (10 days old) were used for the feeding bioassays.

Maize plants

Maize inbred lines MBS847_NLN14 were obtained from Saclay's Divergent Selection Experiments [41]. Seeds were pre-germinated in Sprouting Trays before being transferred into individual pots (4 l) containing Jiffy® premium. Plants were grown in a greenhouse at 16 h light: 8 h darkness with the temperature between 21-24°C and 70% humidity. For the

antifeedant tests controls, leaf disks were taken from mature leaves of the same leaf rank (rank 8). Several plants at the same developmental stage from the same inbred line were used to obtain samples of 50 leaf disks.

Bioassays

Each replicate consisted in 50 disks of 1 cm diameter taken from leaves of the same leaf rank on plants from the same genotype. Approximately 10 leaf disks were sampled on each plant, so that the experiment is not destructive. Leaf disks were deposited on the 50-cages plate onto 1% agarose gel immediately after sampling to avoid dehydration. The bioassays consisted in testing the leaf consumption by the larvae in the presence of two products, an extract from neem seeds, NeemAzal (AMM n° 2140090 *) that contains azadirachtin, and quinine hydrochloride (Sigma Aldrich; CAS number: 6119-47-7) at different concentrations. Leaf disks were sprayed with 10 µl (as spraying volume) of the substance with distilled water as solvent and kept 15 to 20 min at ambient temperature to let the solution dry before starting the experiment. This spraying has been done with repeater sprayer (Repeater ® E3/E3x) on one side of leaf disk. We tested different concentrations of Neemazal (10, 3, 1, 0.1, 0.01 mM) and Quinine (100, 10, 1, 0.1, 0.01 mM). For the control, only 10 µl of distilled water was sprayed. One second instar larva was deposited in each cage. Plates were placed in the monitoring device and larvae were allowed to feed for 48 hours at ambient temperature. At least two replicates (2 plates, i.e. 2 x 50 larvae) were tested for each condition.

Experimental system

Instructions for the making-up of the experimental system are freely available upon request. Plates were designed with AutoCAD software with a 3D printer (Ultimaker 2+) using white PLA (polylactic acid) filament (Ref.RS Stock No. 134-8192), at a resolution of 0,6 mm. Each plate was designed as a plate of 10 x 5 square cages of (13 x 13 x 11 mm) separated by 1 mm

walls. The bottom of the plate was designed with two grooves to slide in a glass plate cut to the corresponding dimensions. The plate was first half-filled with 1% agar solution to maintain leaf disk moisture during the bioassay [21]. One leaf disk and one larva (10 days old) was added in each cage [36]. The top of the plate was then covered with a second glass plate and maintained in place with two rubber bands, to prevent larvae to escape (Fig 1). The webcam was inserted into a stand made from MDF (Medium Density Fiberboard) cut by laser cutting (Fig 1). This stand enclosed an area fitting 3 plates, and ensured that images were taken at the same distance and under the same angle. The plates and the stand were placed on top of an A3 white LED light panel (white 4000K; Display Concept, Brussels, Belgium), lying flat on a table.

Image acquisition and analysis

Image acquisition : Webcams (Logitech Pro C970) were connected to the USB port of a PC computer, with sufficient disk memory to store the images. One standard computer could easily control 4 webcams. Time-lapse images were taken every minute by a video surveillance software (VisionGS BE 3.1.0.4; http://www.visiongs.com) as 1920 x 1080 pixels jpg files, named with a time stamp.

Image analysis : Image analysis of the stacks was performed semi-automatically, with the help of custom programs working within the bio-imaging open-source program ICY (20). In order to follow the consumption of each leaf-disk, regions of interest (ROIs) must first be defined to locate each cage or disk. This is done semi-automatically with a plugin called RoitoRoiArray (http://icy.bioimageanalysis.org/plugin/roitoarray/). Using a combination of image analysis and user input, the plugin generates arrays of ROIs, gives them a unique ID and saves them into an XML file (Figs 2a&b). A second plugin, Areatrack (http://icy.bioimageanalysis.org/plugin/areatrack/), allow users to load stacks of images, browse or display them as a time-lapse movie, and analyse them (Figs 2c&d). After loading the ROIs from the previous file, each image of the stack is filtered and thresholded to keep only the pixels corresponding the leaf areas. Movements of the larvae can also be detected by performing image to image subtraction followed by thresholding. These measures can be then displayed or saved as a CSV file. As considerable variation of lightning and colour of the leaf disks occurred, two detection strategies were implemented. The first approach was to transform the RGB image by transforming it into a grey plane and applying a unique threshold. The filters implemented are: R, G, B, 2R-(G+B), 2G-(R+B), 2B-(R+G), (R+G+B)/3, or converting the image into the HSB space and extracting one component H (HSB), S(HSB) and B (HSB). Although this approach is satisfactory in most cases, some experiments could not be analysed this way. We introduced another approach, which is to let the user point at dots on the screen to build a matrix of colours. These colours were stored either in the RGB, HSV or H1H2H3 space. The user could threshold the image using a distance around these colours, L1 or L2. The distance L1 between colour c1 and c2 is defined in the RGB space as distance

$L1 = |R_{C1} - R_{C2}| + |G_{C1} - G_{C2}| + |B_{C1} - B_{C2}|$. Distance L2 is defined as distance

$$L2 = \sqrt{((R_{C1} - R_{C2})^2 + (G_{C1} - G_{C2})^2 + (B_{C1} - B_{C2})^2)}\ .$$

Both approaches let the user display the thresholded image as an overlay over the original images and thus choose the best adapted threshold. As these experiments generate huge amount of data, additional procedures were implemented behind the screen to fetch data from the disk in advance, and also to explore and analyse only a fraction of the data, for example one image under 10 or under 60. Once the detection was done, by analysing all images of the stack or a subset of them, the resulting data were exported as an excel file, including three type of measures: the raw data (i.e. the number of pixels over the threshold in each cage), a running average and a running median of the raw data using a user-defined span (usually n=10). While this analysis can be run on the three plates at once, it was found usually more convenient to perform the analysis plate by plate (i.e. on a batch of 50 larvae) so that the measures performed on each plate were saved into a one csv file per plate. Although recordings were performed on longer time periods, this paper reports analyses made over a period of time of 48 h, corresponding to stacks of 2,880 images.

Data analysis

Series of R scripts freely available were written for data processing and statistical analysis.

Metadata: Raw files were stored using lab storage facilities on specific directories. Directories names contain information about the date of the experiment and the camera number. Csv filenames contained all the information about the experiment: date, camera ID, plate (from a to f), insect population, plant genotype, plant environment, plant coordinates, substance name, substance concentration. After image analysis, all csv files that are going to be analysed together are copied under a single sub-directory

Standardization: First, raw pdf images of leaf consumption through time are produced. Each pdf file contains 50 plots, one for each cage. Cages that produced abnormal plots, identified by their row and column coordinates, are manually removed from the analysis. Then, we

standardized the data by dividing the leaf area by the total leaf area at time t0. Hence, the basic measure became Y_{tl}, the percentage of intact leaf disk from the cage l at time t. We defined tmax=2500mn (40 hours), and only retained the data taken before tmax.

Data clustering: Because the behaviour of each caterpillar was different, we performed unsupervised clustering [42] on the individual time data using all plates from the same experiment to classify larvae consumptions dynamics into 14 clusters. The total number of clusters was empirically chosen to avoid having clusters containing only a couple of curves and proved to be robust over the different experiments.

Typology of feeding behaviour: Each cluster was characterized by average characteristic times that represented the larvae feeding dynamics of the cluster: t20, t50 and t80 (time after which 20%, 50% and 80% of the leaf disk has been consumed respectively), total consumption of the leaf disk at tmax. Using the K-means algorithm [43], we then arranged the 14 clusters into 6 group of curves, from A to F (Fig 3.4). Each group corresponded to a different feeding behaviour.

Data transformation: At the end of the analysis, each cage l, corresponding to treatment i, batch j and plate k was assigned a unique letter depending on the kind of feeding behaviour of the caterpillar in the cage. The observations of a single cage can be summarized into a vector of zeros and ones $Z_{ijkl} = \left(Z_{ijkl}^{1}, \dots, Z_{ijkl}^{w}, \dots, Z_{ijkl}^{W}\right)$, (1) where w represents one feeding behaviour, with w in {A, B, C, D, E, F}, and $Z_{ijkl}^{w} = 1$ if the observed feeding behaviour is w, and $Z_{ijkl}^{w} = 0$ else.

Statistical analysis: Z_{ijkl} is the result of a multinomial sampling in

$$Z_{ijkl} \equiv M\left(1, p_{ijk}^{1}, \dots, p_{ijk}^{w}, \dots, p_{ijk}^{W}\right) \quad (2)$$

where $P_{ijk}^{w} = P\left(Z_{ijkl}^{w} = w\right)$ is the probability that a single observation falls into the feeding behaviour w. We used the logistic multinomial regression [44] to compare two models using the Akaike Information Criterion (AIC) [45].

In model M1, differences between the observation are due to the treatment i.e. In model M2, differences between observations are due to plate specificities, whatever the treatment. Whenever model M1 is chosen by the AIC criterion means that differences between treatments are greater than differences between plates. A separate analysis was conducted with each molecule (Neemazal and Quinine). Each time model M1 was chosen, we performed a Wald test to compare treatments [46]. The reference W was chosen for each molecule as the feeding type which was the most homogenous between treatments. We chose the feeding type B for plates treated with Quinine, and treatment E for plates treated with Neemazal. The statistical analyses also provided with an estimation of the probabilities associated with each treatment, using $P_i^w = \frac{e^{\mu^w + \alpha_i^w}}{1 + \sum_z e^{\mu^z + \alpha_i^z}}$

Acknowledgments

This work was supported by a scholarship from the Islamic Bank of Development to Inoussa Sanane (N° BID : 600033174) and a grant from the BASC labex (ITEMAIZE project) supported by IDEX Paris-Saclay. We are grateful to Stephane Dallongeville (Institut Pasteur), for his constant help and support for the development of the ICY plugins. We warmly thank members of J Legrand's and F Marion-Poll's laboratories for discussion and support during this work.

Reference

1. Battisti A, Larsson SA, Björkman C, Niemelä P. Climate change and insect pest distribution range. In 2015.

2. Castex V, Beniston M, Calanca P, Fleury D, Moreau J. Pest management under climate change: The importance of understanding tritrophic relations. Science of The Total Environment. 2018;616–617:397–407.academia.edu/40167318

3. Bradshaw CJA, Leroy B, Bellard C, Roiz D, Albert C, Fournier A, et al. Massive yet grossly underestimated global costs of invasive insects. Nature Communications. 2016;7(1): 12986.nature.com/articles/ncomms12986

4. Sakai AK, Allendorf FW, Holt JS, Lodge DM, Molofsky J, With KA, et al. The Population Biology of Invasive Species. Annual Review of Ecology and Systematics.2001;32(1):305–32. doi: 10.1146/annurev.ecolsys.32.081501.114037

5. Little CM, Chapman TW, Hillier NK. Plasticity Is Key to Success of *Drosophila suzukii* (Diptera: Drosophilidae) Invasion. J Insect Sci. 2020 ;20(3). academic.oup.com/jinsectscience/article/20/3/5/5837529

6. Goggin FL, Lorence A, Topp CN. Applying high-throughput phenotyping to plant–insect interactions: picturing more resistant crops. Current Opinion in Insect Science. 2015; 9:69–76.doi: S2214574515000334

7. Jones CG, Coleman JS. Leaf disc size and insect feeding preference: implications for assays and studies on induction of plant defense. Entomologia Experimentalis et Applicata. 1988;47(2):167-72. doi:10.1111/j.1570-7458. 1988.tb01132.

8. Nandy S, Chen Q, Yang J, Beasley D, Li H, Goettel M. Use of a detached leaf screening method for segregating Colorado potato beetle (*Leptinotarsa decemlineata* Say) resistant Solanum hybrid lines. Canadian journal of plant science Revue canadienne de phytotechnie. 2008;88(4): 633-638.doi:10.4141/CJPS07047

9. Visschers IGS, Dam NM van, Peters JL. An objective high-throughput screening method for thrips damage quantitation using Ilastik and ImageJ. Entomologia Experimentalis et Applicata. 2018;166(6):508–15.doi:10.1111/eea.12682

10. Arnason JT, Philogène BJR, Donskov N, Hudon M, McDougall C, Fortier G, et al. Antifeedant and insecticidal properties of azadirachtin to the European Corn Borer, *Ostrinia nubilalis*. Entomologia Experimentalis et Applicata. 1985;38(1):29–34. doi:10.1111/j.1570-7458. 1985.tb03494.x

11. Belles X, Camps F, Coll J, Piulachs MD. Insect antifeedant activity of clerodane diterpenoids against larvae of *Spodoptera littoralis* (Boisd.) (Lepidoptera). J Chem Ecol. 1985;11(10):1439–45. doi:10.1007/BF01012143

12. Yencho GC, Renwick JAA, Steffens JC, Tingey WM. Leaf surface extracts of *Solanum berthaultii* hawkes deter colorado potato beetle feeding. J Chem Ecol. 1994;20(5):991–1007. doi:10.1007/BF02059737

13. Shields VDC, Rodgers EJ, Arnold N, Williams D. Feeding responses to selected alkaloids by gypsy moth larvae, *Lymantria dispar* (L.). Naturwissenschaften. 2006;93(3):127–30.ncbi.nlm.nih.gov/pmc/articles/PMC2970768/

14. Guthrie WD, Dicke FF, Neiswander CR. Leaf and sheath feeding resistance to the European corn borer in eight inbred lines of dent corn. 1960; kb.osu.edu/handle/1811/62651

15. Isman MB, Koul O, Luczynski A, Kaminski J. Insecticidal and antifeedant bioactivities of neem oils and their relationship to azadirachtin content. J Agric Food Chem. 1990 ;38(6):1406–11.doi:10.1021/jf00096a024

16. Escoubas P, Lajide L, Mitzutani J. An improved leaf-disk antifeedant bioassay and its application for the screening of Hokkaido plants. Entomologia Experimentalis et Applicata. 1993;66(2):99–107.doi:10.1111/j.1570-7458. 1993.tb00697.x

17. Alchanatis V, Navon A, Glazer I, Levski S. PA—Precision Agriculture: An Image Analysis System for measuring Insect Feeding Effects caused by Biopesticides. Journal of Agricultural Engineering Research. 2000 ;77(3):289–96.doi: S0021863400906103

18. Rowley M, Stitt J, Hanson F. Image analysis of small animal feeding behavior. Behavior Research Methods, Instruments, & Computers. 2003;35(3):447–51. doi:10.3758/BF03195522

19. Ji CW, Park C-G, Lee S-W, Kim J-H, Choi BR. Continuous measuring of leaf area for analyzing feeding behavior of *Spodoptera litura* (Lepidoptera: Noctuidae) larva. Journal of Asia-Pacific Entomology. 2017;20(2):491–5. doi: S1226861516303508

20. Chaumont F de, Dallongeville S, Chenouard N, Hervé N, Pop S, Provoost T, et al. Icy: an open bioimage informatics platform for extended reproducible research. Nature Methods. 2012 ;9(7):690–6.com/articles/nmeth.2075

21. Jin S. Maize defense responses to caterpillars at the molecular, phenotypic and ecological scales. [PhD Thesis]. Pennsylvania State University; 2017.

22. Schmutterer H. Potential of azadirachtin-containing pesticides for integrated pest control in developing and industrialized countries. Journal of Insect Physiology. 1988 ;34(7):713–9. doi:0022191088900820

23. Mordue (Luntz) AJ, Blackwell A. Azadirachtin: an update. Journal of Insect Physiology. 1993;39(11):903–24. doi:0022191093900018

24. Lowery DT, Isman MB. Insect growth regulating effects of neem extract and azadirachtin on aphids. Entomologia Experimentalis et Applicata. 1994;72(1):77–84. doi:10.1111/j.1570-7458. 1994.tb01804.x

25. Bezzar-Bendjazia R, Kilani-Morakchi S, Maroua F, Aribi N. Azadirachtin induced larval avoidance and antifeeding by disruption of food intake and digestive enzymes in *Drosophila melanogaster* (Diptera: Drosophilidae). Pestic Biochem Physiol. 2017; 143:135–40.

26. Ruiz-Mesia L, Ruiz-Mesía W, Reina M, Martínez-Diaz R, de Inés C, Guadaño A, et al. Bioactive Cinchona Alkaloids from *Remijia peruviana*. J Agric Food Chem. 2005 ;53(6):1921–6. doi:10.1021/jf048880e

27. Sellier M-J, Reeb P, Marion-Poll F. Consumption of bitter alkaloids in *Drosophila melanogaster* in multiple-choice test conditions. Chem Senses. 2011;36(4):323–34.

28. Minnich DE. An experimental study of the tarsal chemoreceptors of two nymphalid butterflies. Journal of Experimental Zoology. 1921;33(1):172–203. doi:10.1002/jez.1400330105

29. Ramaswamy SB, Cohen NE, Hanson FE. Deterrence of feeding and oviposition responses of adult *Heliothis virescens* by some compounds bitter-tasting to humans. Entomologia

Experimentalis et Applicata. 1992;65(1):81–93. doi:10.1111/j.1570-7458. 1992.tb01630.x

30. Shikano I, Akhtar Y, Isman MB, Rankin CH. Dishabituating long-term memory for gustatory habituation in the cabbage looper, *Trichoplusia ni*. Behav Neurosci. 2010 ;124(5):701–5.

31. Salloum A, Colson V, Marion-Poll F. Appetitive and Aversive Learning in *Spodoptera littoralis* Larvae. Chem Senses. 2011;36(8):725–31. doi:36/8/725/266361

32. Pszczolkowski MA. Pharmacological analysis of the feeding response of codling moth (*Cydia pomonella*; Lepidoptera: Tortricidae) neonates to bitter compounds. 2017;

33. Mebs D, Wunder C, Toennes SW. Coping with noxious effects of quinine by praying mantids (Mantodea) and spiders (Araneae). Toxicon. 2019; 162:57–60. doi: S0041010119300959

34. Städler E, Schöni R. High sensitivity to sodium in the sugar chemoreceptor of the cherry fruit fly after emergence. Physiological Entomology. 1991;16(1):117–29. doi:10.1111/j.1365-3032. 1991.tb00548.x

35. Sandoval M, Albert PJ. Chemoreception of sucrose and amino acids in second and fourth instars of the spruce budworm *Choristoneura fumiferana* (Clem.) (Lepidoptera: Tortricidae). Journal of Insect Physiology. 2007;53(1):84–92. doi: S0022191006001855

36. Menezes Jr. AO, Oliveira A, Mikami AY, Ide AK, Ventura MU. Feeding preferences of *Microtheca punctigera* (Achard) (Coleoptera: Chrysomelidae) for some Brassicaceae plants in multiple-choice assays. Scientia Agricola. 2005;62(1):72–5. doi: S0103-90162005000100014

37. Clark EL, Isitt R, Plettner E, Fields PG, Huber DPW. An Inexpensive Feeding Bioassay Technique for Stored-Product Insects. Journal of Economic Entomology. 2014;107(1):455–61.doi:10.1603/EC13283

38. O'Neal ME, Landis DA, Isaacs R. An Inexpensive, Accurate Method for Measuring Leaf Area and Defoliation Through Digital Image Analysis. J Econ Entomol. 2002 ;95(6):1190–4. doi:95/6/1190/863513

39. Huang J, Nuessly GS, McAuslane HJ, Nagata RT. Effect of screening methods on expression of romaine lettuce resistance to adult banded cucumber beetle, *Diabrotica balteata* (coleoptera: chrysomelidae). Florida Entomologist. 2003;86(2):194–8.

40. Vigneault C, Barkiré B, Martel P. Méthode de mesure de surface de feuilles utilisée dans l'évaluation d'insecticides. Cahiers Agricultures. 1995;4(1):53-55 (1).

41. Aguirre-Liguori JA, Gaut BS, Jaramillo-Correa JP, Tenaillon MI, Montes-Hernández S, García-Oliva F, et al. Divergence with gene flow is driven by local adaptation to temperature and soil phosphorus concentration in teosinte subspecies (*Zea mays* parviglumis and *Zea mays* mexicana). Molecular Ecology. 2019;28(11):2814–30. doi:10.1111/mec.15098

42. Herrero J, Valencia A, Dopazo J. A hierarchical unsupervised growing neural network for clustering gene expression patterns. Bioinformatics. 2001;17(2):126–36. doi:17/2/126/182096

43. Hartigan JA, Wong MA. Algorithm AS 136: A K-Means Clustering Algorithm. Journal of the Royal Statistical Society Series C (Applied Statistics). 1979;28(1):100–8. doi:2346830

44. Venables WN, Ripley BD. Modern Applied Statistics with S. 4th ed. New York: Springer-Verlag; 2002. (Statistics and Computing). doi:9780387954578

45. Akaike H. Information Theory and an Extension of the Maximum Likelihood Principle. In: Parzen E, Tanabe K, Kitagawa G, editors. Selected Papers of Hirotugu Akaike. New York, NY: Springer; 1998. p. 199–213. (Springer Series in Statistics). doi:10.1007/978-1-4612-1694-0_15

46. Davidson R, Mackinnon JG. 'The Method of Maximum Likelihood: Fundamental Concepts and Notation'. Estimation and Inference in Econometrics. New York: Oxford University Press. p. 89. 1993.doi: qed.econ.queensu.ca/ETM/etm-info.html

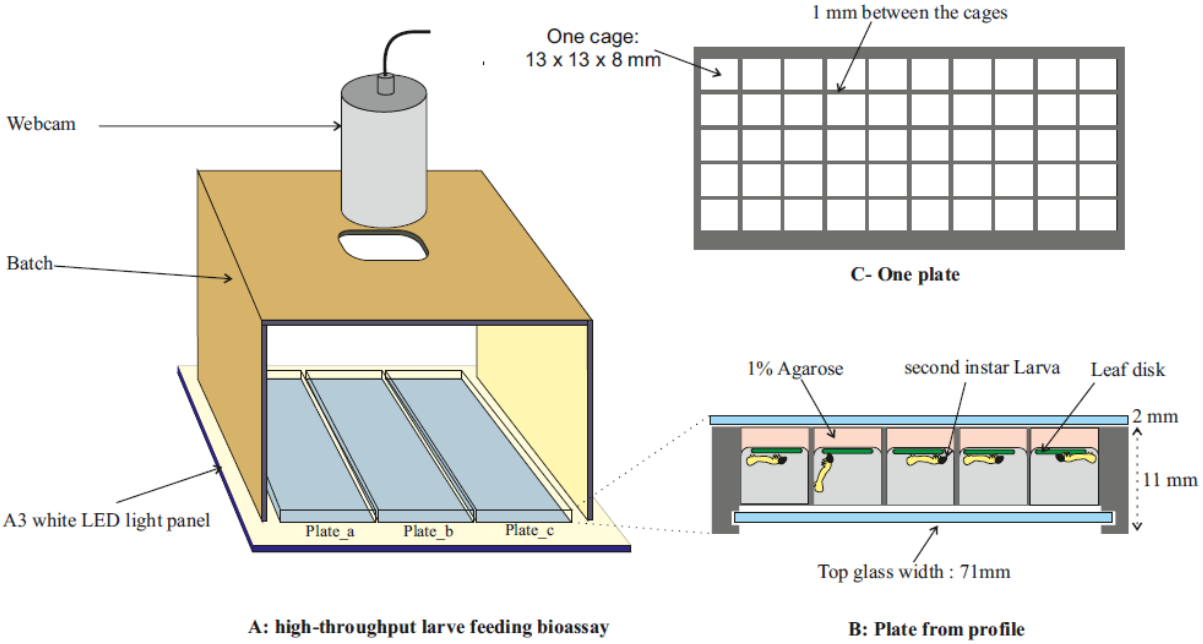
Webcam
Batch
A3 white LED light panel
Plate_a
Plate_b
Plate_c
One cage:
13 x 13 x 8 mm
1 mm between the cages
C- One plate
1% Agarose
second instar Larva
Leaf disk
2 mm
11 mm
Top glass width : 71mm
A: high-throughput larve feeding bioassay
B: Plate from profile

Figure 1.

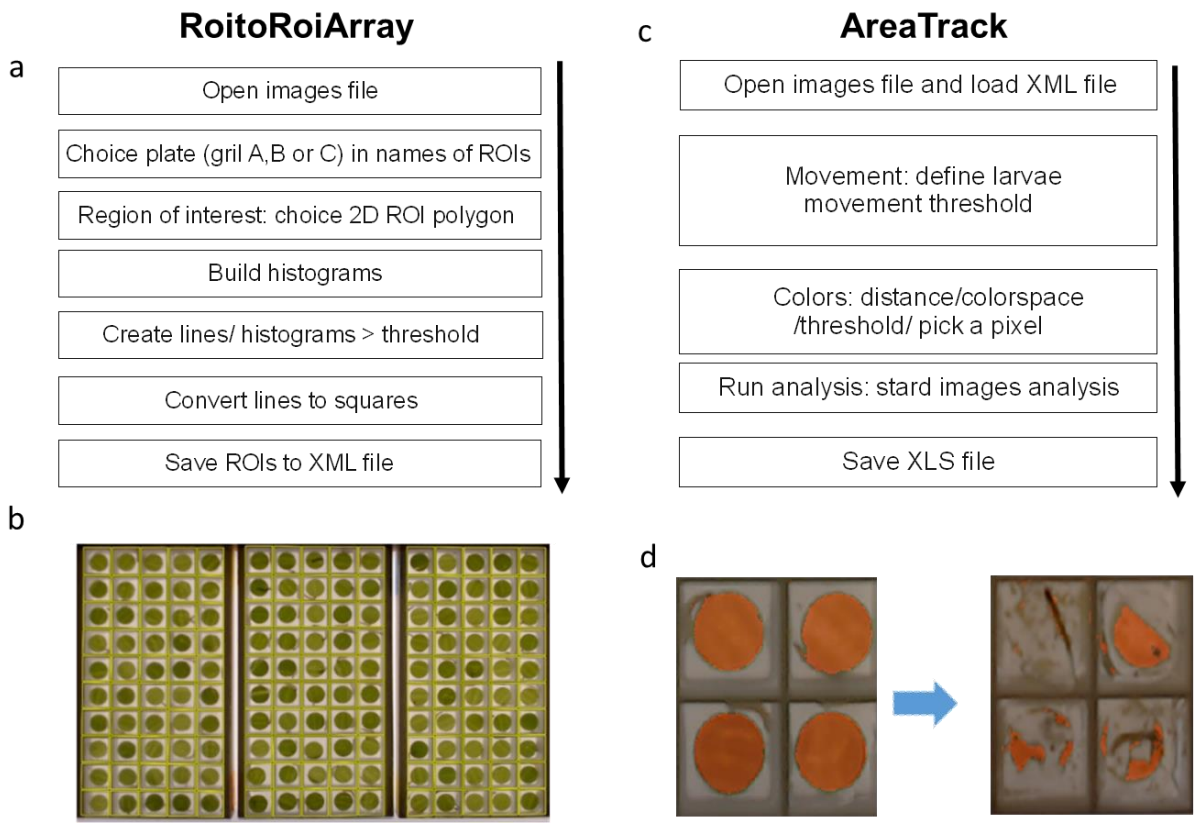
RoitoRoiArray
a
Open images file
Choice plate (gril A,B or C) in names of ROIs
Region of interest: choice 2D ROI polygon
Build histograms
Create lines/ histograms > threshold
Convert lines to squares
Save ROIs to XML file
b
c
AreaTrack
Open images file and load XML file
Movement: define larvae movement threshold
Colors: distance/colorspace /threshold/ pick a pixel
Run analysis: stard images analysis
Save XLS file
d

Figure 2.

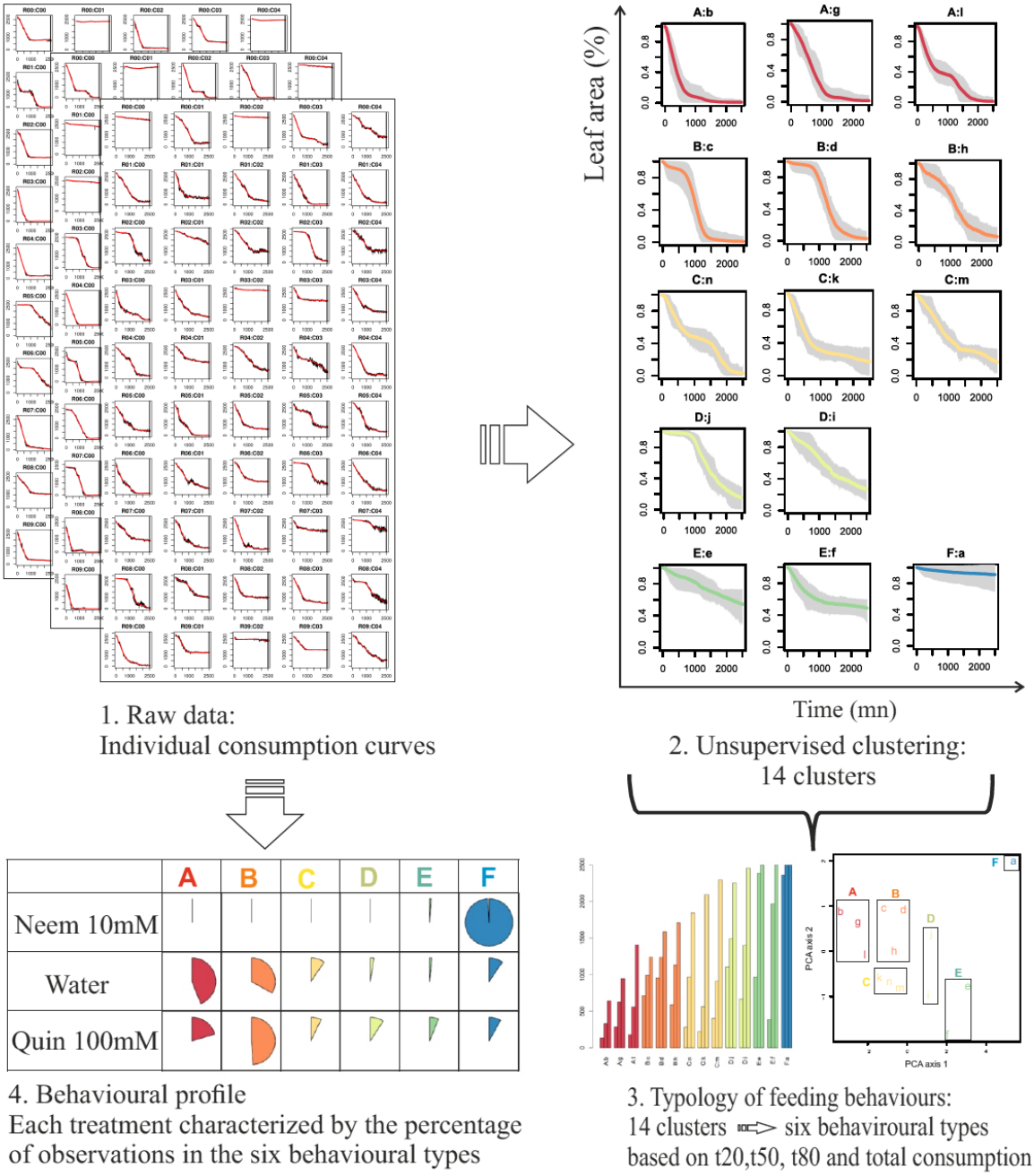
Leaf area (%)
Time (mn)
A:b
A:g
A:l
B:c
B:d
B:h
C:n
C:k
C:m
D:j
D:i
E:e
E:f
F:a
1. Raw data:
Individual consumption curves
2. Unsupervised clustering:
14 clusters
A
B
C
D
E
F
Neem 10mM
Water
Quin 100mM
PCA axis 1
PCA axis 2
4. Behavioural profile
Each treatment characterized by the percentage
of observations in the six behavioural types
3. Typology of feeding behaviours:
14 clusters ⇨ six behaviroural types
based on t20,t50, t80 and total consumption

Figure 3.

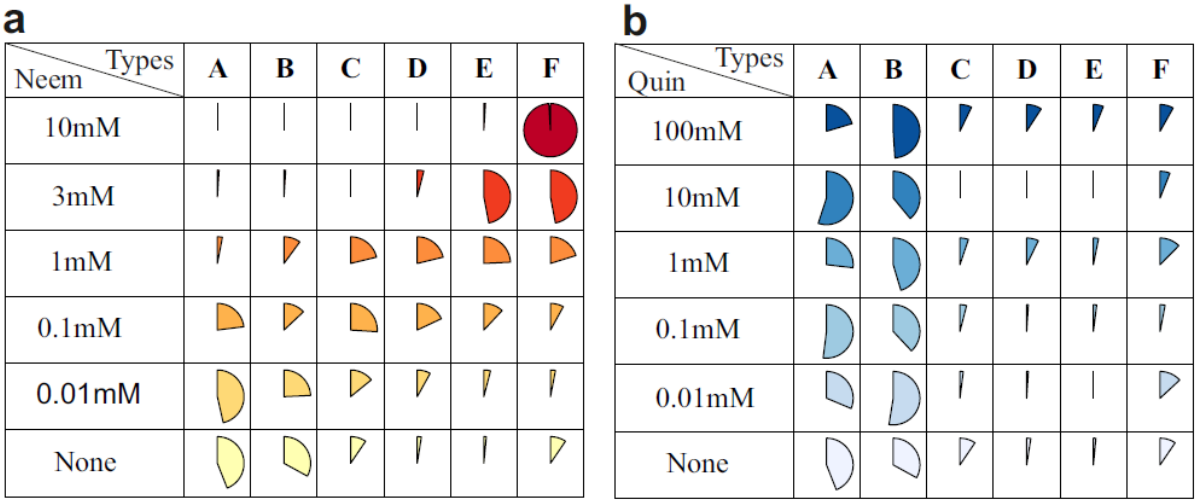
a
Types
Neem
A
B
C
D
E
F
10mM
3mM
1mM
0.1mM
0.01mM
None
b
Types
Quin
A
B
C
D
E
F
100mM
10mM
1mM
0.1mM
0.01mM
None

Figure 4.